Journal of Advances in Computer Research
Quarterly pISSN: 2345-606x eISSN: 2345-6078
Sari Branch, Islamic Azad University, Sari, I.R.Iran
(Vol. 10, No. 1, February 2019), Pages: 25-42
www.jacr.iausari.ac.ir

Determination of a New Model to Study Ultra-Saturation Phenomenon During the Loaded Power Transformer Energization and its Effect on Differential

Bahram Noshad✉
Department of Electrical Engineering, Bandar Deylam Branch, Islamic Azad University, Bandar Deylam, Iran
bahramnoshad@yahoo.com

Received: 2018/05/06; Accepted: 2018/09/01

Abstract

One of transient phenomenon that causes the mal-operation of the power transformer differential protection during the energization of a loaded power transformer is the ultra-saturation phenomenon. In this paper, a new model for investigating the ultra-saturation phenomenon during the energization of a loaded power transformer is presented and its effect on the differential protection of the power transformer is considered. In this model, the nonlinear characteristic of the power transformer core, the effect of current transformers, and the core losses of the power transformer are taken into account. It is assumed that the load of the power transformer is a resistive and inductive load. Also, the effect of the residual flux and inception angle on the ultra-saturation phenomenon are investigated. In this paper, simulation is done by MATLAB software. The differential protection of the power transformer must be accurate and fast, so the description of the ultra-saturation phenomena is the first level for preventing of the mal-operation of the differential protection. The outcomes of this research can further be used as hints for substation operation personnel as well as for the development of new protection stabilization criteria, which is not discussed further in this paper.

Keywords: *Power Transformer, Differential Protection, Inrush Current, Ultra-Saturation Phenomenon, False Trip*

1. Introduction

Large power transformers are of the most important parts in power systems and the differential protection of the power transformers is a major concern [1]. The effect of the magnetizing inrush currents has to consider in the power transformer protective design [2]. The magnetizing inrush current includes high level of second harmonic component which is used as a discriminative feature in conventional protective schemes [1, 2]. Normally, in order to distinguish between the external faults, internal faults and magnetizing inrush current, an algorithm is used in which the differential protection operates when the amplitude of the basic component of the differential current fixes upper than 0.25p.u and the level of the second harmonic to basic harmonic of the differential current fixes lower than 15% [3-8]. But it has been described that in certain conditions the mal-operation of differential protection under magnetizing inrush current leaded to tripping of healthy transformers [5-7]. In [5-7], the mal-operation of

differential protection during the energization of the loaded transformer was reported whose extraction is known as ultra-saturation phenomenon. The mechanism of unusual mal-operation of the differential protection due to the ultra-saturation phenomenon is related to saturation of the magnetic core of the power transformer which is occurred during a rapid jump of the terminal voltages that is a famous and studied phenomenon. It happens when a power transformer is switched on or after removing a short circuit fault that occurred nearby a power transformer. In these satiations, it may create slow and high decaying inrush currents that may be much higher than the full load value [9-11]. In [5], many simplifications during the simulations are carried out which take the magnetizing reactance of the time-variant characteristic as an equivalent inductance, neglecting the core model of the transformer, without considering the transferring effect of current transformer to the primary inrush, and consider only the resistive load, can be mentioned which does not correspond with the real status. Hanli Weng et al. revised their previous model in 2007. According to them the previous theory cannot be used to study the ultra-saturation phenomenon. So, a new model for studying the ultra-saturation phenomenon during the loaded power transformer energization, with the current transformer model including the effect of the magnetic hysteresis, taking the nonlinear magnetizing reactance, and no considering only the resistive load is proposed [6]. But in [6], the core losses of the transformer are neglected and a difficult model for current transformer in primary side is considered whose main difficulty in current transformer modeling is the hysteresis loop simulation. Andrzej Wiszniewski et al. the conditions which must be discovered to make ultra-saturation phenomenon and excessive ultra-saturation phenomenon possible are presented in 2008 [7]. In [7], the ATP-EMTP program is used for simulation. For determining the conditions that discovered ultra-saturation and excessive ultra-saturation phenomenon in [7], the core model of the power transformer and the magnetizing reactance are ignored, therefore this does not correspond with the real status.

In this paper, a new model for investigating the ultra-saturation phenomenon during the energization of a loaded power transformer is presented and its effect on the differential protection of the power transformer is considered. In this model, the nonlinear characteristic of the power transformer core, the effect of current transformers, and the core losses of the power transformer are taken into account. It is assumed that the load of the power transformer is a resistive and inductive load. In addition to a new model for the power transformer, a very simple, accurate and effective model for the current transformer is presented in this paper. The main advantages of this proposed model to investigate the ultra-saturation for power transformer and current transformers in compare with previous models are 1) the core losses of the power transformer are taken into account, 2) In the power transformer and current transformer models, information of B-H curve for magnetic branch is not required, 3) Hysteresis effect isn't taken into account and Compliance with the IEEE model with considering hysteresis effect [12], 4) the proposed model can be compared to the single-valued magnetization characteristic model proposed by the IEEE Power System Relaying Committee (PSRC) [12-13] and 5) It involves proper computing speed and accuracy. Also, the mal-operation of the differential protection depends on a variety of factors the most important parameters of which are residual flux and inception angle. In this paper the parameters mentioned will be studied in various scenarios. The differential protection of the power transformer must be accurate and fast, so the description of the ultra-saturation phenomena is the first level for preventing of the mal-operation of the

differential protection. In this paper, the equations are solved by fourth-order Runge-Kutta technique and simulation is done by MATLAB software.

The paper is organized as follows. Section 2 introduces the modeling of the ultra-saturation phenomenon. Section 3 presents a new model for the current transformer. Simulation results of the ultra-saturation phenomenon are presented in section 4. Finally, Conclusions are given in section 5.

2. Ultra-Saturation Phenomenon Modelling

The equivalent circuit of the loaded power transformer energization is shown in Figure 1.

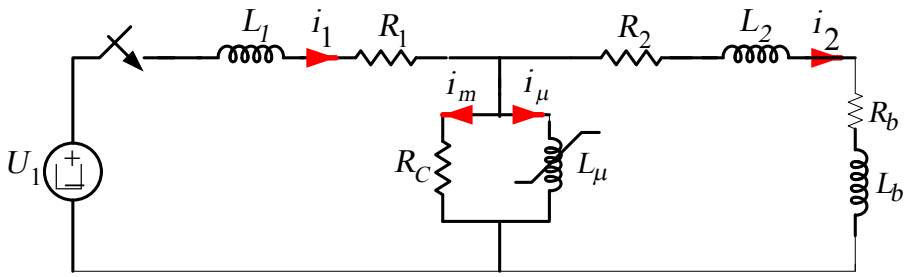

Figure 1. Electrical equivalent circuit of the loaded transformer energization with considering core model

In this model, U_1 is the electromotive force of the source, L_1 and R_1 represent the inductive and the resistive components of the equivalent impedance comprising of system impedance and leakage impedance of the transformer primary winding. L_2 and R_2 represent the inductive and resistive components of the equivalent impedance comprising of the leakage impedance of transformer secondary winding. L_b and R_b are the inductive and resistive components of the burden impedance of power transformer. The magnetizing nonlinear branch of transformer core is illustrated by an equivalent inductance L_μ and R_c is represented iron loss of power transformer. For modeling of the loaded power transformer, the equivalent circuit illustrated in Figure 1 is considered. In this circuit, we defined:

$$R = R_2 + R_b$$
$$L = L_2 + L_b \quad (1)$$

According to equivalent circuit of transformer in figure 1:

$$\frac{d\psi_1}{dt} + R_1 i_1 + \frac{d\psi_\mu}{dt} = U_1 \quad (2)$$

$$\frac{d\psi_\mu}{dt} = \frac{d\psi_2}{dt} + R i_2 \quad (3)$$

$$i_1 = i_2 + i_\mu + i_m \quad (4)$$

In these equations, i_1 and i_2 are the currents of the primary side and the secondary side of the power transformer, respectively. ψ_1 and ψ_2 are the induced magnetic linkage according to i_1 and i_2. i_μ is the current of transformer magnetizing branch and ψ_μ is

induced magnetic linkage according to i_μ. For the linear branches of the equivalent circuit of the power transformer, the primary current and secondary current are defined as follows:

$$i_1 = \psi_1 / L_1 \, , i_2 = \psi_2 / L \tag{5}$$

i_m is the branch current concern the core loss according to which the equivalent circuit of transformer, can be defined as (6).

$$i_m = \frac{1}{R_c} \frac{d\psi_\mu}{dt} \tag{6}$$

According to (4) and (6):

$$i_2 = i_1 - i_\mu - \frac{1}{R_c} \frac{d\psi_\mu}{dt} \tag{7}$$

Substitute (5) and $i_\mu = f(\psi_\mu)$ into (7), (8) can be obtained as follows:

$$\psi_2 = \frac{L}{L_1} \psi_1 - Lf(\psi_\mu) - \frac{L}{R_c} \frac{d\psi_\mu}{dt} \tag{8}$$

In (8) $f(\psi_\mu) = i_\mu$ is concern the nonlinear magnetizing branch current. The exact curve of $\psi_\mu - i_\mu$ should be shown as a multi-valued curve if the hysteresis is considered. But according to previous studies, since the hysteresis characteristic does not considerably affect the power transformer and current transformer transient behavior [12, 14-15], the magnetization curve shown in Figure 2 is considered. In others words, this single-valued magnetization curve is used for the power transformer and the current transformer, Since the hysteresis characteristic does not considerably affect the power transformer and current transformer transient behavior, therefore single-valued curve is appropriate curve for transient analysis and can be used instead of multi-valued curve. In Figure 2, it can be assumed that the saturation point is (i_{μ_0}, ψ_s). In this paper, the approximate magnetization curve shown in Figure 2 is used for power transformer and current transformer that ψ_s and i_{μ_0} are different for the power transformer and the current transformer. The inductance in saturation region and no saturation region are L_s and L_μ, respectively. It should be accented that the inductance of the magnetizing branch of the power transformer is nonlinear yet, even though the mentioned simplification is used. Hence, according to Figure 2 i_μ can be defined as follow:

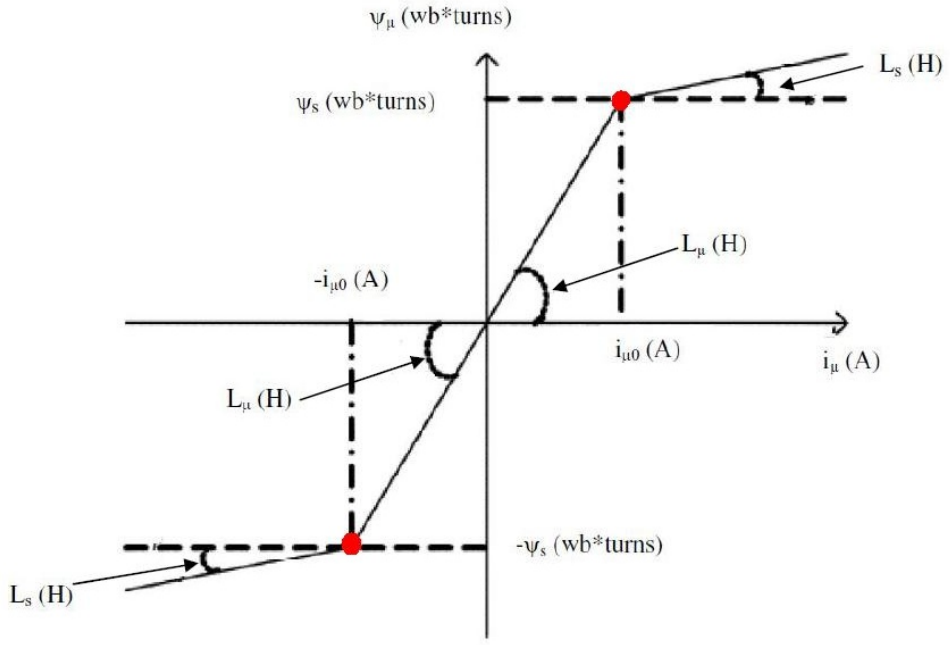

Figure 2. The approximate magnetizing characteristic of transformer core [5-7]

$$i_\mu = \begin{cases} \dfrac{\psi_\mu - \psi_s}{L_s} + i_{\mu 0} & \psi_\mu > \psi_s \\ \dfrac{\psi_\mu + \psi_s}{L_s} - i_{\mu 0} & \psi_\mu < -\psi_s \\ i_{\mu 0}\dfrac{\psi_\mu}{\psi_s} & |\psi_\mu| \le \psi_s \end{cases} \tag{9}$$

In equation (9), ψ_μ represents the flux linkages of the power transformer, ψ_s represents the flux linkages at the saturation knee point of the magnetization curve of the power transformer, $i_{\mu 0}$ represents the magnetization current at the saturation knee point of the magnetization curve of the power transformer and L_s represents the slope of the saturation curve.

Substitute $i_1 = \psi_1 / L_1$ into (2), (10) can be obtained as follow:

$$\frac{d\psi_1}{dt} + R_1\frac{\psi_1}{L_1} + \frac{d\psi_\mu}{dt} = U_1 \tag{10}$$

Substitute (4), (6), and (8) into (3), (11) can be obtained as follow:

$$\frac{d\psi_\mu}{dt} = \frac{L}{L_1}\frac{d\psi_1}{dt} - L\frac{df(\psi_\mu)}{dt} - \frac{L}{R_c}\frac{d^2\psi_\mu}{dt^2} + R\frac{\psi_1}{L_1} - Ri_\mu - \frac{R}{R_c}\frac{d\psi_\mu}{dt} \tag{11}$$

According to (10), (12) can be obtained as follow:

$$\frac{d\psi_1}{dt} = U_1 - R_1 \frac{\psi_1}{L_1} - \frac{d\psi_\mu}{dt} \tag{12}$$

Substitute (12) into (11), (13) can be obtained as follow:

$$\frac{d\psi_\mu}{dt} = \frac{L}{L_1} U_1 - \frac{LR_1}{L_1^2}\psi_1 - \frac{L}{L_1}\frac{d\psi_\mu}{dt} - L\frac{df(\psi_\mu)}{dt} - \frac{L}{R_c}\frac{d^2\psi_\mu}{dt^2} + R\frac{\psi_1}{L_1} - Ri_\mu - \frac{R}{R_c}\frac{d\psi_\mu}{dt} \tag{13}$$

According to Figure 2, the magnetization curve of the power transformer has three regions.

If $\psi_\mu > \psi_s$:

In this case the magnetization current is defined:

$$i_\mu = \frac{(\psi_\mu - \psi_s)}{L_s} + i_{\mu 0} \tag{14}$$

$$\frac{df(\psi_\mu)}{dt} = \frac{d(i_\mu)}{dt} = \frac{1}{L_s}\frac{d\psi_\mu}{dt} \tag{15}$$

Substitute (14) and (15) into (13), (16) can be obtained as follow:

$$\begin{aligned} &\frac{d^2\psi_\mu}{dt^2} + \frac{d\psi_\mu}{dt}\left(\frac{R_c}{L} + \frac{R_c}{L_1} + \frac{R_c}{L_s} + \frac{R}{L}\right) + \psi_\mu\left(\frac{RR_c}{LL_s}\right) + \frac{RR_c}{L} i_{\mu 0} - \frac{RR_c}{LL_s}\psi_s \\ &+ \psi_1\left(\frac{R_1 R_c}{L_1^2} - \frac{RR_c}{L_1 L}\right) = \frac{R_c}{L_1} U_1 \end{aligned} \tag{16}$$

If $\psi_\mu < -\psi_s$:

In this case the magnetization current is defined:

$$i_\mu = \frac{1}{L_s}(\psi_\mu + \psi_s) - i_{\mu 0} \tag{17}$$

Substitute (15) and (17) into (13), (18) can be obtained as follow:

$$\begin{aligned} &\frac{d^2\psi_\mu}{dt^2} + \frac{d\psi_\mu}{dt}\left(\frac{R_c}{L} + \frac{R_c}{L_1} + \frac{R_c}{L_s} + \frac{R}{L}\right) + \psi_\mu\left(\frac{RR_c}{LL_s}\right) - \frac{RR_c}{L} i_{\mu 0} + \frac{RR_c}{LL_s}\psi_s \\ &+ \psi_1\left(\frac{R_1 R_c}{L_1^2} - \frac{RR_c}{L_1 L}\right) = \frac{R_c}{L_1} U_1 \end{aligned} \tag{18}$$

If $|\psi_\mu| \le \psi_s$:

In this case the magnetization current is defined:

$$i_\mu = i_{\mu 0}\frac{\psi_\mu}{\psi_s} \tag{19}$$

Substitute (14) and (19) into (12), (20) can be obtained as follow:

$$\frac{d^2\psi_\mu}{dt^2}+\frac{d\psi_\mu}{dt}\left(\frac{R_c}{L}+\frac{R_c}{L_1}+\frac{R_c i_{\mu 0}}{\psi_s}+\frac{R}{L}\right)+\psi_\mu\left(\frac{R_c R i_{\mu 0}}{L\psi_s}\right)+\psi_1\left(\frac{R_1 R_c}{L_1^2}-\frac{RR_c}{L_1 L}\right)=\frac{R_c}{L_1}U_1 \quad (20)$$

3. Modeling of the Current Transformer

In this paper, a new model is presented for current transformer which is very simple and effective. The current transformer equivalent circuit and referred to the secondary side are shown in Figures 3 and 4. In these circuits R_1 and L_1 are the resistive and the inductive components of the equivalent impedance comprising of system impedance and leakage impedance of the transformer primary winding. R_2 and L_2 are resistive and inductive of the secondary side of the current transformer. R_b and L_b are resistive and inductive burden of the current transformer. Since the core loss doesn't affect the behavior of the current transformer saturation, it is ignored [16]. Figure 4 is shown the current transformer model referred to secondary side. In this Figure, the magnetizing branch of the current transformer is nonlinear and for nonlinear magnetizing branch of current transformer Figure 2 is considered. Therefore, according to Figure 2, the magnetizing branch is defined as equation (9) and to model the current transformer, following equations are described according to Figure 4. In the following equations, equation (9) is utilized for magnetizing branch current. In other hands, the approximate magnetization curve shown in Figure 2 is used for current transformer that ψ_s and $i_{\mu 0}$ are different for the power transformer and the current transformer. To model the current transformer, equivalent circuit shown in Figure 4 is considered. In this circuit, we defined:

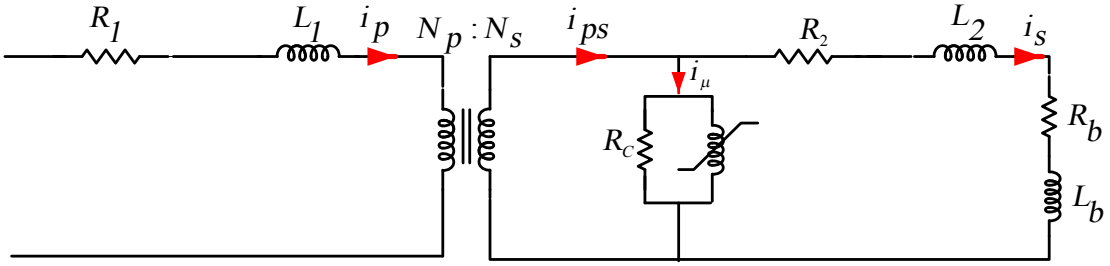

Figure 3. The current transformer model

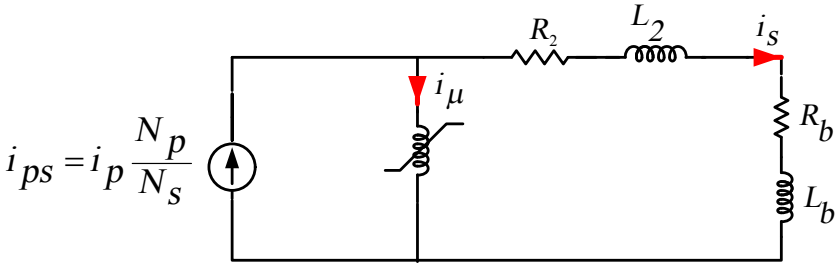

Figure 4. The current transformer model referred to secondary side

$$R = R_2 + R_b$$
$$L = L_2 + L_b \quad (21)$$

According to the equivalent circuit shown in Figure 4:

$$i_{ps} = i_\mu + i_s \quad (22)$$

$$e_s = Ri_s + L\frac{di_s}{dt} \quad (23)$$

$$i_{ps} = \frac{N_p}{N_s} i_p \quad (24)$$

In these equations i_{ps} represents the primary current that referred to the secondary side, i_μ is the magnetizing current, i_s is the secondary current, N_p is the number of primary turns, N_s is the number of secondary turns, and e_s represents the induced voltage in the secondary winding. According to (22):

$$i_s = i_{ps} - i_\mu \quad (25)$$

According to Figure 2 and equation (9), the magnetization curve of the current transformer has three regions.

If $\psi_\mu > \psi_s$:

In this case the magnetization current is defined:

$$i_\mu = \frac{(\psi_\mu - \psi_s)}{L_s} + i_{\mu_0} \quad (26)$$

According to (25) and (26):

$$i_s = i_{ps} - \frac{1}{L_s}(\psi_\mu - \psi_s) - i_{\mu_0} \quad (27)$$

Differentiate from (27):

$$\frac{di_s}{dt} = \frac{di_{ps}}{dt} - \frac{1}{L_s}\frac{d\psi_\mu}{dt} \quad (28)$$

Due to $\frac{d\psi_\mu}{dt} = e_s$ from (23), (27) and (28):

$$\frac{d\psi_\mu}{dt} = \frac{RL_s}{L_s + L}\left(i_{ps} - \frac{(\psi_\mu - \psi_s)}{L_s} - i_{\mu_0}\right) + \frac{LL_s}{L_s + L}\left(\frac{di_{ps}}{dt}\right) \quad (29)$$

If $\psi_\mu < -\psi_s$:

In this case the magnetization current is defined:

$$i_\mu = \frac{1}{L_s}(\psi_\mu + \psi_s) - i_{\mu_0} \quad (30)$$

According to (25) and (30):

$$i_s = i_{ps} - \frac{1}{L_s}(\psi_\mu + \psi_s) + i_{\mu_0} \quad (31)$$

Differentiate from (31):

$$\frac{di_s}{dt} = \frac{di_{ps}}{dt} - \frac{1}{L_s}\frac{d\psi_\mu}{dt} \quad (32)$$

Due to $\frac{d\psi_\mu}{dt} = e_s$ from (23), (31) and (32):

$$\frac{d\psi_\mu}{dt} = \frac{RL_s}{L_s + L}(i_{ps} - \frac{(\psi_\mu + \psi_s)}{L_s} + i_{\mu_0}) + \frac{LL_s}{L_s + L}(\frac{di_{ps}}{dt}) \quad (33)$$

If $|\psi_\mu| \le \psi_s$:

In this case the magnetization current is defined:

$$i_\mu = i_{\mu_0} \frac{\psi_\mu}{\psi_s} \quad (34)$$

According to (25) and (34):

$$i_s = i_{ps} - i_{\mu_0} \frac{\psi_\mu}{\psi_s} \quad (35)$$

Differentiate from (35):

$$\frac{di_s}{dt} = \frac{di_{ps}}{dt} - \frac{i_{\mu_0}}{\psi_s}\frac{d\psi_\mu}{dt} \quad (36)$$

Due to $\frac{d\psi_\mu}{dt} = e_s$ from (23), (35) and (36):

$$\frac{d\psi_\mu}{dt} = \frac{R\psi_s}{\psi_s + i_{\mu_0}}(\frac{N_p}{N_s} i_{ps} - i_{\mu_0} \frac{\psi_\mu}{\psi_s}) + \frac{L\psi_s}{\psi_s + i_{\mu_0}}(\frac{N_p}{N_s}\frac{di_{ps}}{dt}) \quad (37)$$

4. Simulation Results

It is supposed that the loaded power transformer is switched on from the high-voltage side at $t = 0$. ψ_μ and ψ_1 can be solved from (10), (16), (18), and (20) by using the forth-order Runge-Kutta technique with a 1μs time step. The Figure 5 displays the curve of the magnetic linkage in the core of power transformer after transformer energization. The magnetic current i_μ according to (9), the primary current according to $i_1 = \psi_1 / L_1$ and the secondary current according to (7) have been calculated using the computed ψ_μ and ψ_1 that are shown in Figures 6, 7, and 8, respectively.

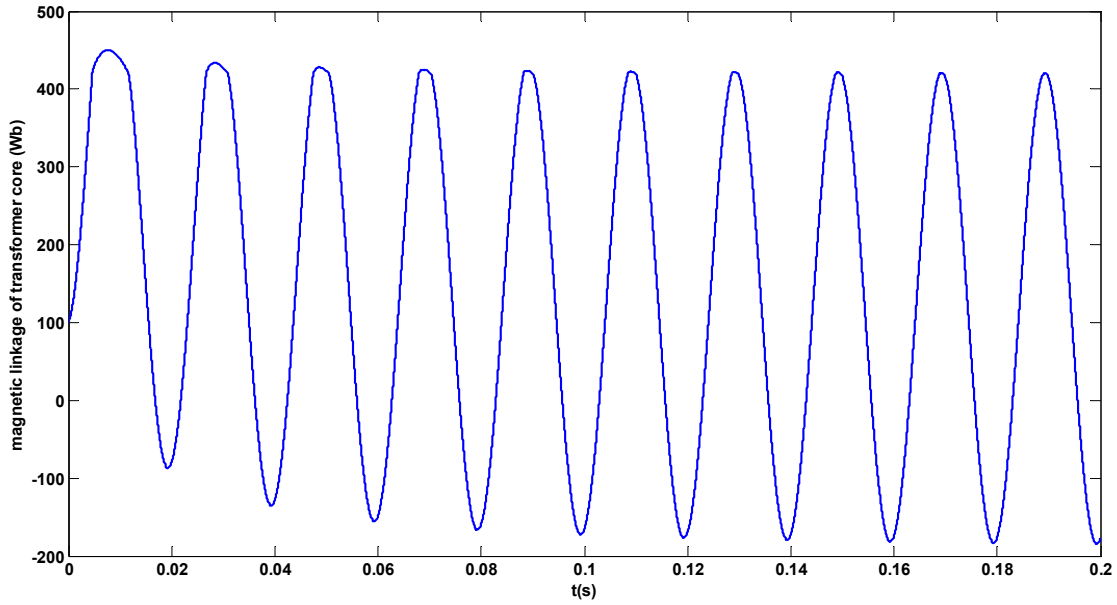

Figure 5. Wave shape of the magnetic linkage of the power transformer core

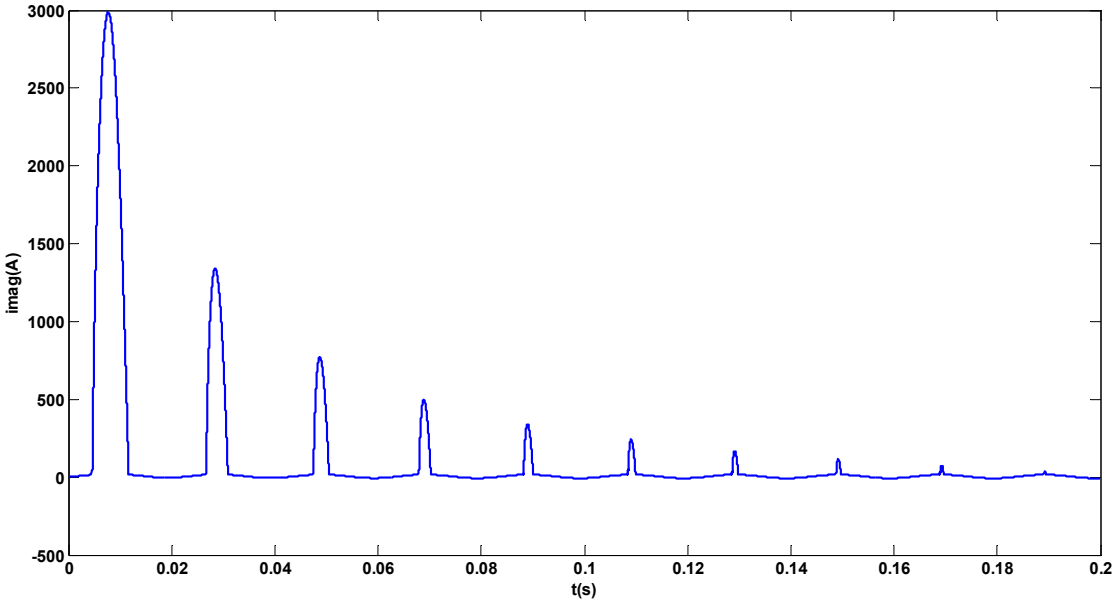

Figure 6. Wave shape of the current of the power transformer magnetizing branch

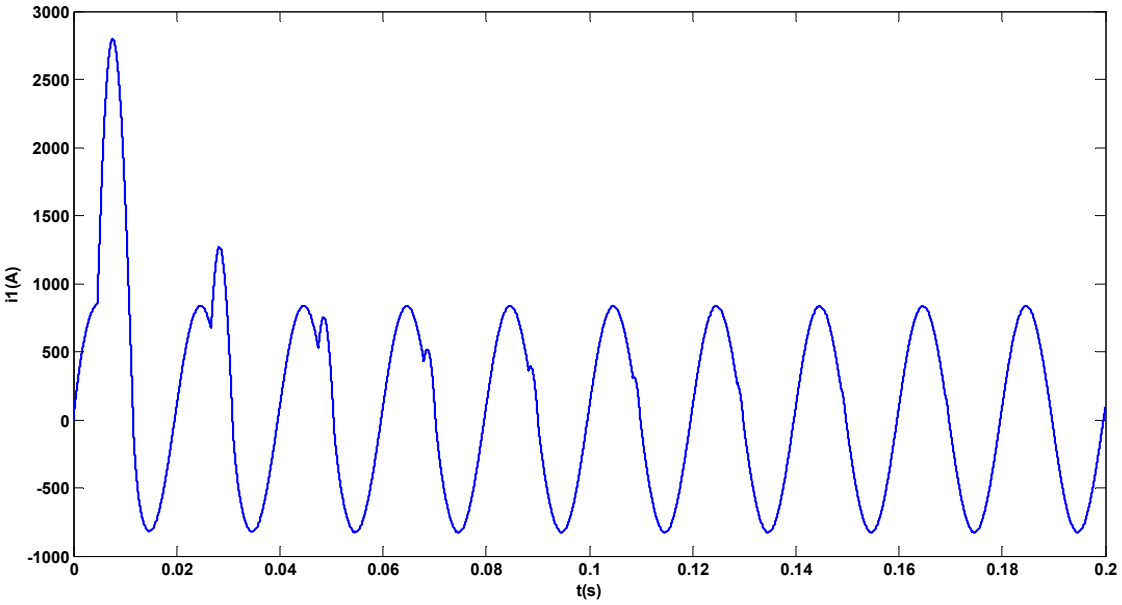

Figure 7. Wave shape of the primary current of the power transformer

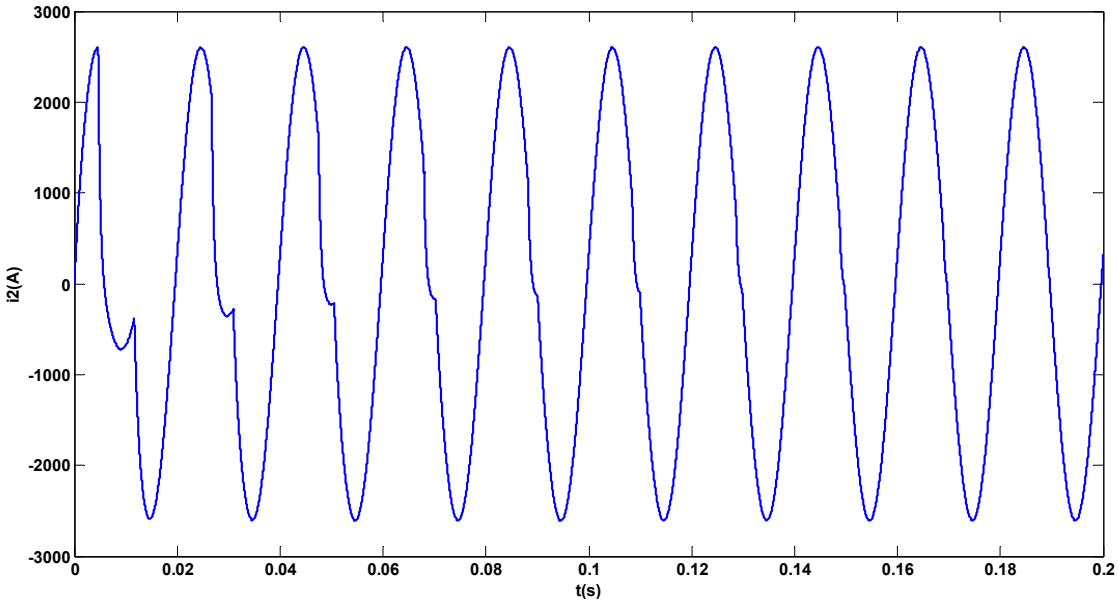

Figure 8. Wave shape of the secondary current of the power transformer

i_1 is the primary current of the power transformer and the current transformer on the primary side of power transformer and i_2 is the secondary current of the power transformer and primary current of the current transformer on the secondary side of the power transformer. Now the secondary currents of the current transformers on the primary and secondary side of the power transformer should be achieved. ψ_μ is related to current transformers on the primary and secondary side of the power transformer and can be solved from (29), (33) and (37) by using the forth-order Runge-Kutta technique

with a 1μs time step. The magnetic current i_μ according to (9) and the secondary current of current transformers according to given (27), (31) and (35) have been calculated using the computedψ_μ. In these relations, i_{ps} is the primary current of the power transformer. With considering primary current for the input of the current transformer in the primary side of power transformer, the route of dynamic magnetizing of the current transformer on the primary side of power transformer is shown in Figure 9. In Figure 10, the primary current refers to the secondary side and the secondary current of the current transformer on the primary side of the power transformer are shown, that are i_{11} and i_{12} respectively. In Figure 11, the primary current refers to the secondary side and the secondary current of the current transformer on the secondary side of the transformer are shown, that are i_{21} and i_{22} respectively. The magnetizing currents of current transformers on the primary and secondary sides can be obtained from subtraction the primary current refers to secondary side and secondary current of current transformer which are shown in the Figures 12 and 13. According to these Figures, The magnetizing current of the current transformer on the primary side involves much higher aperiodic component because of the nonlinearity of the transformer core, but the aperiodic component on the current transformer on the secondary side of the power transformer is greatly low.

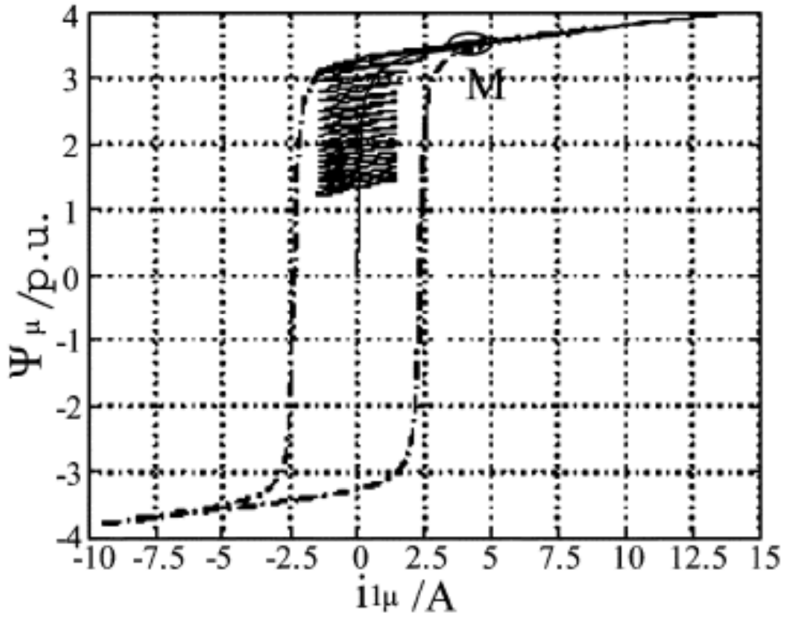

Figure 9. the rouse of dynamic magnetizing of the current transformer at the primary side of power transformer [6]

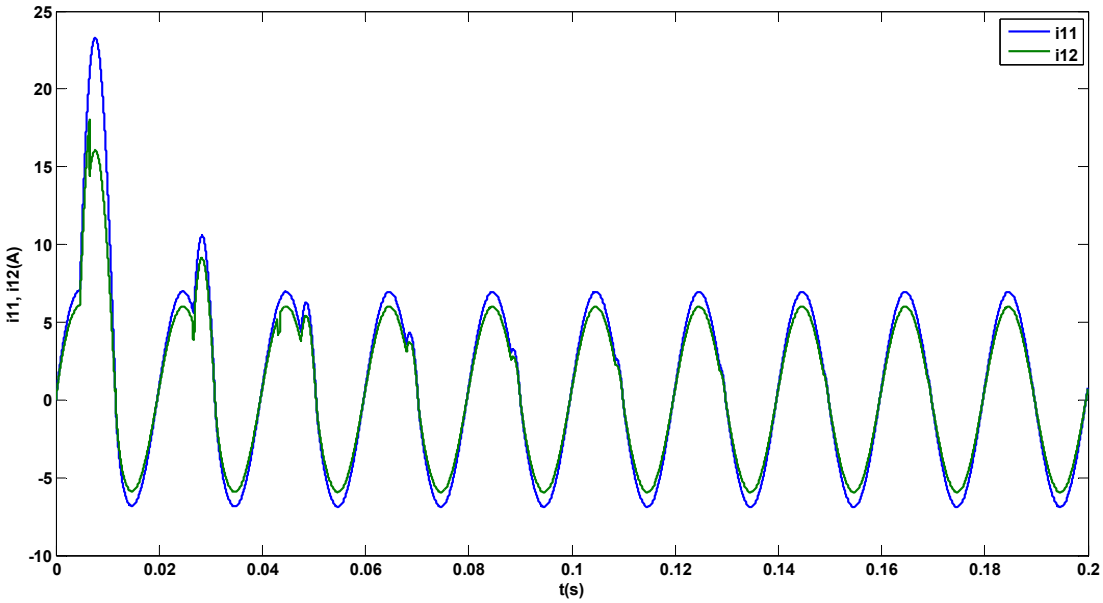

Figure 10. The primary current refers to the secondary side and the secondary current of the current transformer on the primary side of the power transformer

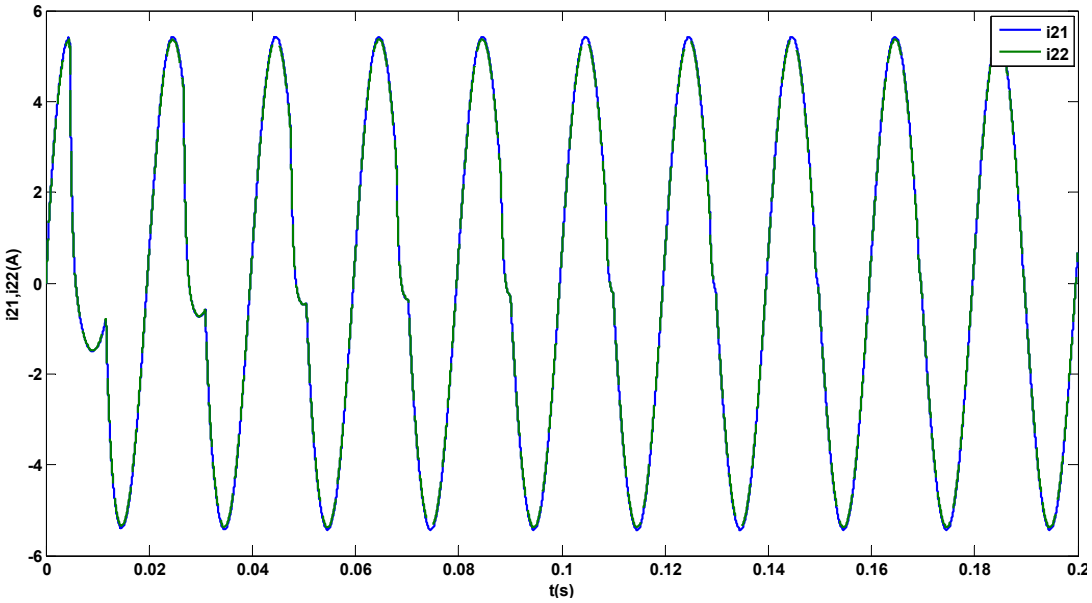

Figure 11. The primary current refers to the secondary side and the secondary current of the current transformer on the secondary side of the power transformer

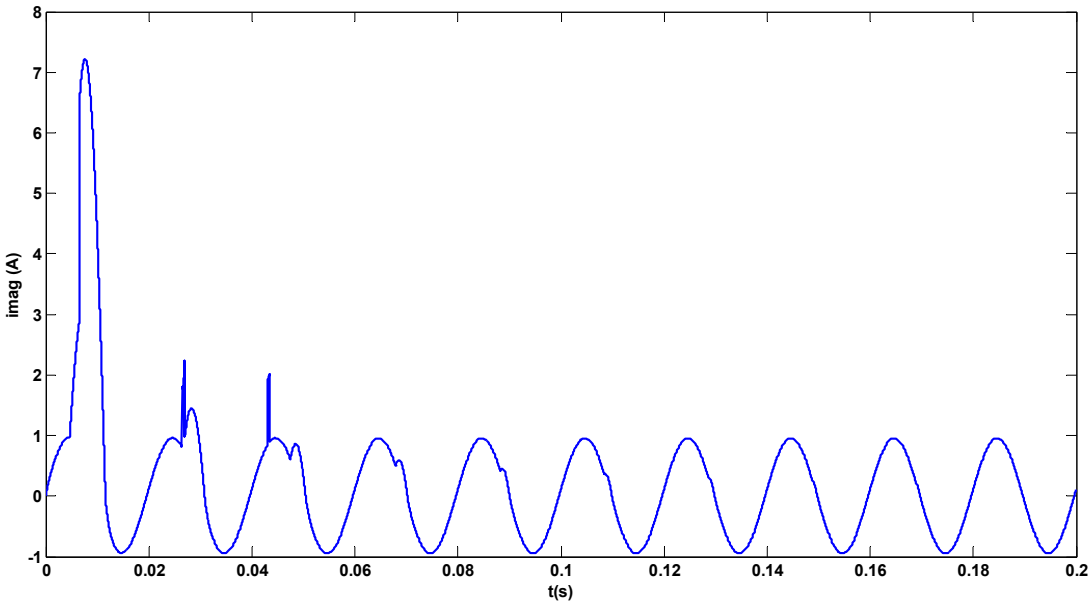

Figure 12. the magnetizing current of the current transformer on the primary side of the power transformer

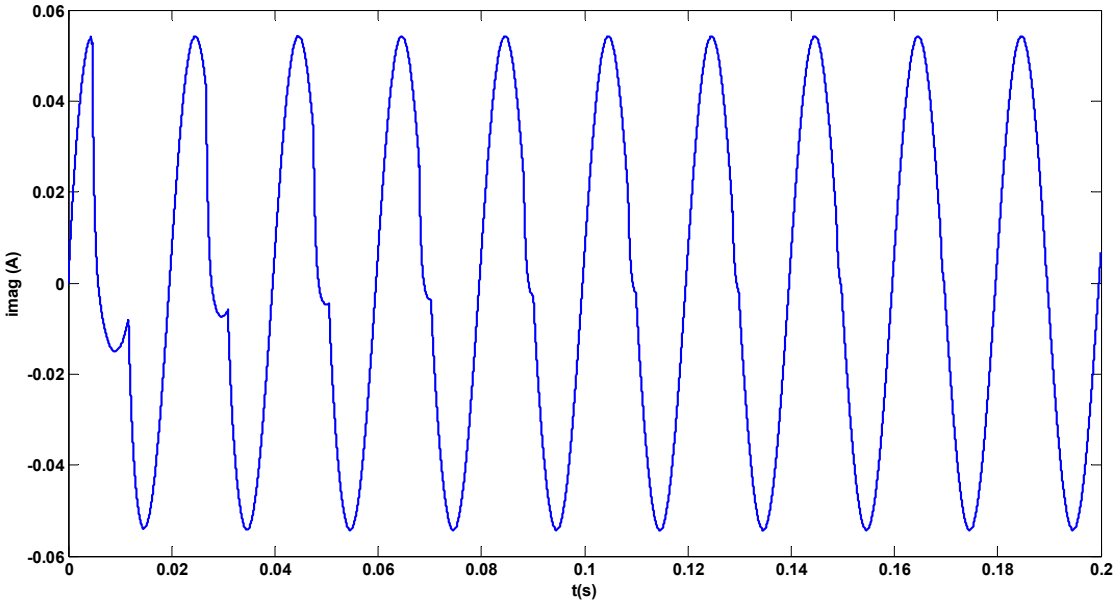

Figure 13. the magnetizing current of the current transformer on the secondary side of the power transformer

Also the differential current ($\dot{I}_d$) shown in Figure 14 can be obtained from subtract i_{12} and i_{22}. As illustrated in Figures 10 and 11, the primary current of the power transformer involves much higher aperiodic component because of the nonlinearity of the transformer core, but the aperiodic component on the secondary current of the power transformer is greatly low. In this case, the current transformers of primary and secondary sides of the power transformer in the transforming behavior differ so greatly

that the false differential current (Figure 14) with considerable magnitude and low harmonic contents will probably be created.

If the amplitude of the basic component of the differential current fixes upper than 0.25p.u. and the level of the second harmonic to basic harmonic of the differential current fixes lower than 15%, the differential protection will operate. Figure 15 displays the changes of the amplitude of the basic component of differential current in Figure 14 that is obtained with the Discrete Fourier Transform method. In this Figure, the amplitude of the basic component of the differential current is normalized according to the secondary current of current transformers. Figure 15 can be compared to Figures 10 and 15 in [6]. As illustrated in Figure15, the basic component of differential current is upper than 0.25p.u from the beginning of energization and approximately, after five cycles it is fixed on 0.2617p.u. and at final (*t=0.2s*), it is fixed on 0.2531p.u. that supported the accuracy of results.

Figure 16 displays the ratio change of the second harmonic to basic harmonic of the differential current ($\dot{I}_d$) after energization that is obtained with the Discrete Fourier Transform method.

As illustrated in Figure15, the basic component of differential current is upper than 0.25p.u from the beginning of energization and approximately, after five cycles it is fixed on 0.2617p.u. According to Figure16, if the energization time exceeds 0.1111s, the ratio of the second harmonic to basic harmonic fixes lower than 15%. If the differential protection utilize 0.25p.u. as the operating threshold and utilized 15% as the second harmonic to the basic harmonic restraint level, the mal-operation of differential protection happens at 0.1111s. All obtained results can be compared to references [5-7].

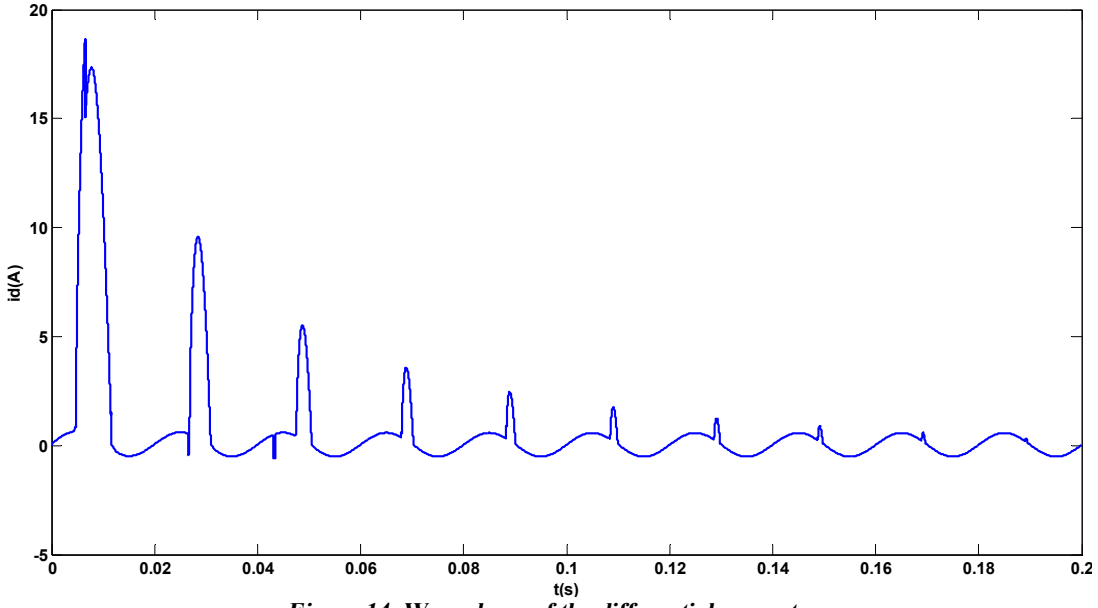

Figure 14. Wave shape of the differential current

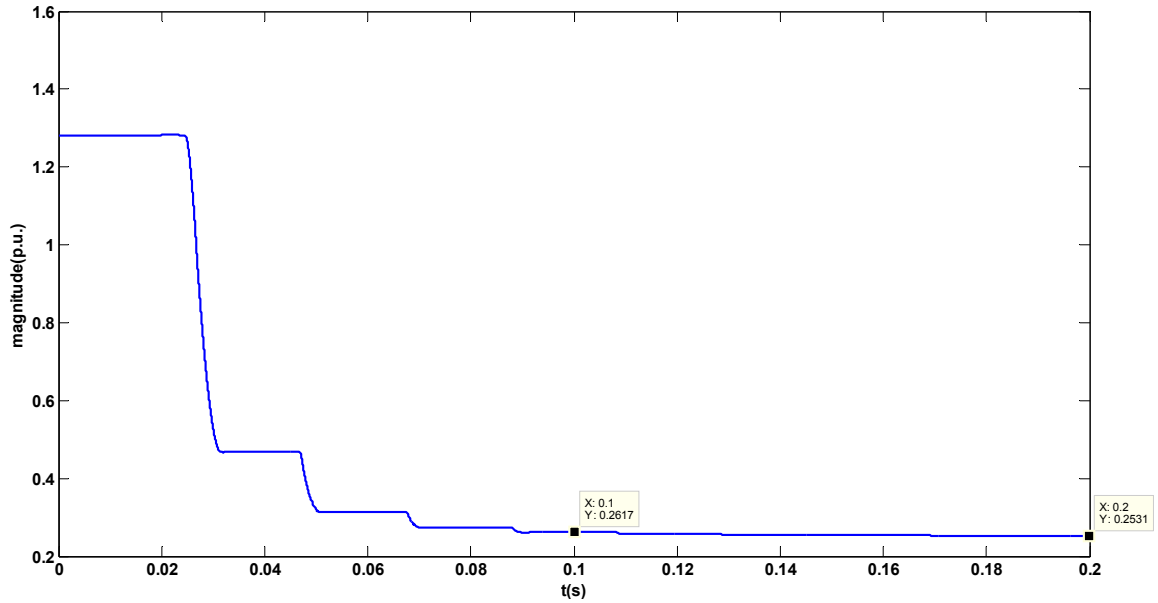

Figure 15. Wave shape of the normalized amplitude of the basic component of the differential current with Discrete Fourier Transform method

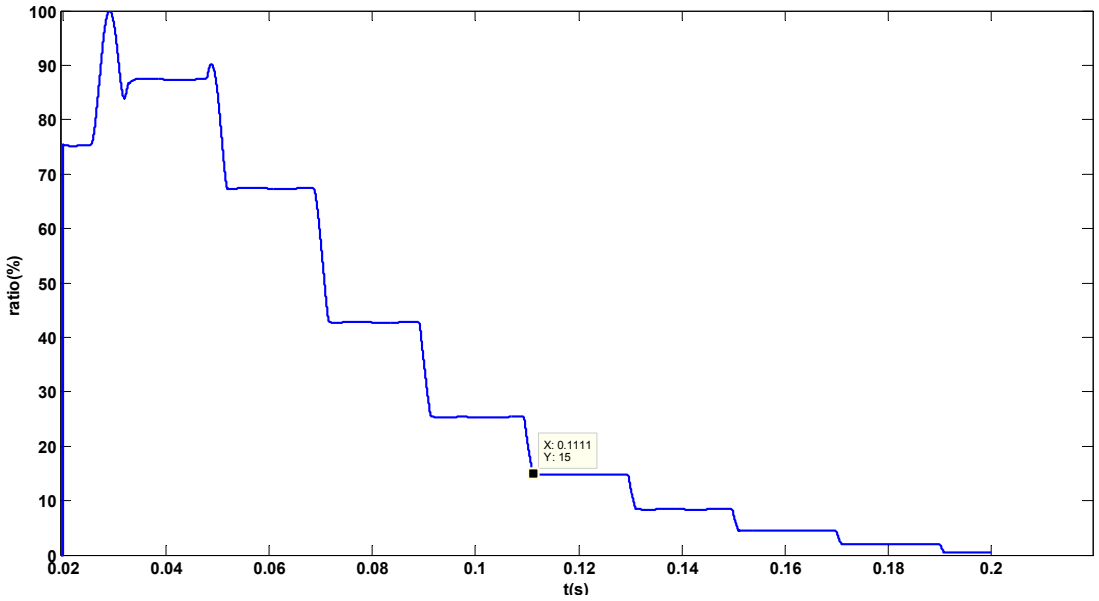

Figure 16. Wave shape of the ratio of second harmonic to basic harmonic component of the differential current with Discrete Fourier Transform method

Also, the occurrence of the delayed mal-operation of the differential protection depends on a variety of factors that the most important which can be noted residual flux and inception angle. In the previous simulations the inception angle was 20 degrees and the residual flux was 100 Webbers as shown in Figure 5. In tables 1 and 2, various scenarios for different inception angles and residual fluxes are presented, respectively. In tables 1 and 2, m ،t_a ، t_{trip} are the amplitude of reaching the basic component of the differential current to five cycles (0.1s), the time of reaching the ratio of the second

harmonic to the basic harmonic of the differential current to 15% and the time of the differential protection tripping, respectively. According to table 1, the worst cases of inrush happen in inception angle of zero and as the inception angle increases, the time of the differential protection decreases. As shown in table 2, if residual flux increases, time of the differential protection increases.

Table 1: Various scenarios for different inception angles

θ $(^\circ)$	$\psi_\mu(0)$ (wb)	m $(p.u.)$	t_a (s)	t_{trip} (s)
0	100	0.262	0.1123	0.1123
20	100	0.2617	0.1111	0.1111
40	100	0.2606	0.1099	0.1099
60	100	0.2583	0.1081	0.1081
80	100	0.2541	0.1056	0.1056

Table 2: Various scenarios for different residual fluxes

$\psi_\mu(0)$ (wb)	θ $(^\circ)$	m $(p.u.)$	t_a (s)	t_{trip} (s)
-100	20	0.2559	0.1094	0.1094
-50	20	0.2578	0.1098	0.1098
0	20	0.2594	0.1102	0.1102
50	20	0.2606	0.1108	0.1108
100	20	0.2617	0.1111	0.1111

5. Conclusion

In this paper, a new model for investigating the ultra-saturation phenomenon during the energization of a loaded power transformer was presented and its effect on the differential protection of the transformer was considered. In this model, the nonlinear characteristic of the power transformer core, the effect of current transformers, and the core losses of the power transformer were also taken into account. It was assumed that the load of the transformer is a resistive and inductive load. In addition to a new model for the power transformer, a very simple, accurate and effective model for the current transformer was presented in this paper. Also, the mal-operation of the differential protection depends on a variety of factors the most important parameters of which are residual flux and inception angle. Finally, the parameters mentioned were studied in various scenarios. The results showed that the ultra-saturation was a probably phenomenon.

References

[1] C. A. Mathews, "An improved transformer differential relay", AIEE Trans., pt. III, vol. 73, pp. 645–650, Jun. 1954.

[2] T. R. Specht, "Transformer magnetizing inrush current", AIEE Trans., pt. I, vol. 70, pp. 323–328, 1951.

[3] A. Wiszniewski, H. Ungrad, and W. Winkler, "Protection Techniques in Electrical Energy Systems", New York: Marcel Dekker, 1995.

[4] "Numerical Differential Protection Relay for Transformers, Generators, Motors and Mini Bus bars", SIEMENS AG, 2006, 7UT613/63x V.4.06 Instruction Manual, Order. C53000-G1176-C160-2.

[5] X. Lin, P. Liu, "The Ultra-Saturation Phenomenon of Loaded Transformer Energization and Its Impacts on Differential Protection", IEEE Transactions on power delivery, Vol. 20, No. 2, april 2005.

[6] H. Weng, X. Lin, and P. Liu, "Studies on the Operation Behavior of Differential Protection during a Loaded Transformer Energization", IEEE Transactions on power delivery, Vol. 22, No. 3, july 2007.

[7] A. Wiszniewski, W. Rebizant, D. Bejmert, and L. Schiel, "Ultra saturation Phenomenon in Power Transformers—Myths and Reality", IEEE Transactions on power delivery, Vol. 23, No. 3, july 2008.

[8] B. Noshad, "A New Model for Analysis of Unusual Mal-Operation of Differential Protection Due to the Ultra-Saturation Phenomenon during the Loaded Power Transformer Energization", Journal of Advances in Computer Research, 2018.

[9] M. Taghipour, S. M. Razavi, and M. A. Shamsinejad, "Intelligent Determining Amount of Inter-Turn Stator Synchronous Motor Using an Artificial Neural Network Trained by Improved Gravitational Search Algorithm", Journal of Advances in Computer Research, 2014.

[10] M. Taghipour, M. Yazdani, S. A. Gholamian, and M. Razavi, "A Novel Approach for Discrimination Magnetizing Inrush Current and Internal Fault in Power Transformers Based on Neural Network", Journal of Advances in Computer Research, 2014.

[11] S. M. B. Sadati, J. Moshtagh, A. Rastgou, "Load and Harmonic Forecasting for Optimal Transformer Loading and Life Time by Artificial Neural Network", Journal of Advances in Computer Research, 2015.

[12] A. Rezaei, R. Iravani, M. Sanaye-Pasand, H. Mohseni, S. Farhangi, "An Accurate Current Transformer Model Based on Preisach Theory for the Analysis of Electromagnetic Transients", IEEE Transactions on Power Delivery, vol. 23, no. 1, pp. 233–242, 2008.

[13] IEEE Power System Relaying Committee, "CT Saturation Theory and Calculator", Working Group Rep, 2001.

[14] A. Hooshyar, S. Afsharnia, M. Sanaye-Pasand, B. Ebrahimi, "A New Algorithm to Identify Magnetizing Inrush Conditions Based on Instantaneous Frequency of Differential Power Signal", IEEE Transactions on Power Delivery, vol. 4, no. 1, pp. 2223-33, 2010.

[15] D. Cwry, P. Icampo, M. Tavm, "Modeling a Power Transformer for Investigation of Digital Protection Schemes", the 8th International Conference on Harmonics and Qualify of Power ICHQP, Greece, October 14-1 6, 1998.

[16] M. Naidu, G. Swift, "Dynamic Analysis of a current Transformer during Faults", Electric Power System Research, 11(1986) 225-231.